DOI: 10.1021/ma101790q

Macromolecules
ARTICLE

Copolymerization of VDF and HFP in Supercritical Carbon Dioxide: Experimental Analysis of the Reaction Loci

L. Ivano Costa,[†,‡] Giuseppe Storti,[†] Massimo Morbidelli,[†] Loredana Ferro,[‡] Onofrio Scialdone,[‡] Giuseppe Filardo,[‡] and Alessandro Galia*[,‡]

[†]*Institute for Chemical and Bioengineering, Swiss Federal Institute of Technology Zürich, ETHZ,Wolfgang-Pauli-Strasse 10, 8093 Zürich, Switzerland, and* [‡]*Dipartimento Ingegneria Chimica Processi e Materiali, Università di Palermo, Viale delle Scienze, Ed.6, 90128 Palermo, Italy*

Received August 5, 2010; Revised Manuscript Received October 24, 2010

ABSTRACT: Free radical copolymerization reactions of vinylidene fluoride (VDF) and hexafluoropropylene (HFP) were carried out in supercritical carbon dioxide at $T = 50$ °C. When ammonium carboxylate perfluoropolyether surfactants were used, the formation of polymer particles was observed provided that HFP mole fraction in the feed was not larger than 0.30. Under these conditions, the effect of the total interphase area of the polymer phase, A_p, on the product properties was investigated by comparing experiments with largely different amounts of stabilizer, i.e., ranging from precipitation (smaller A_p) to dispersion (larger A_p) polymerization systems. We found that the copolymer molecular weight distribution (MWD) is heavily affected by A_p. This experimental evidence strongly supports the presence of two reaction sites, the CO_2-rich and the polymer-rich phase: the contribution of both is important in the examined range of operating conditions.

1. Introduction

Fluoropolymers are macromolecules of choice when severe environmental conditions require high thermal and chemical stability.[1,2] These features are due to the presence of fluorine atoms as substituents and are coupled with good mechanical and dielectric properties and low surface energy.[3,4] Vinylidene fluoride−hexafluoropropylene (VDF−HFP) random copolymers are an important class of such materials. Their properties can be tuned from those of a semicrystalline thermoplastic to those of a fully amorphous elastomer by increasing the HFP content. Commercial VDF−HFP copolymers reach a maximum of 22−23 mol % in HFP and are mainly used in the production of tubing, valves, and fittings.[1,2,5] Moreover, PVDF membranes are used for protein immunoblot[6,7] due to their low affinity for amino acids. Low content HFP copolymers (up to 5 mol %) showed interesting properties, when properly processed, in the preparation of membranes for fuel cell applications.[8,9]

The industrial production of VDF−HFP copolymers is nowadays based on aqueous emulsion or suspension processes,[2] generating large amount of wastewater and requiring high energy for drying. Their production is thus associated with environmental issues that could be overcome by replacing water with the "green" solvent supercritical carbon dioxide ($scCO_2$) as dispersing medium: CO_2 is in fact cheap, nontoxic, and nonflammable, does not undergo chain transfer reactions, and, being a gas at ambient conditions, dry polymer is easily obtained upon depressurization of the system. Several recent works showed that this is in fact a promising alternative to traditional polymerization solvents,[10] and the first industrial plant for the production of tetrafluoroethylene fluoropolymers in $scCO_2$ is operated by DuPont for several years.[11,12]

Working above or below the polymer cloud point at the selected operating conditions, the synthesis of VDF-based polymers in $scCO_2$ can be carried out in homogeneous[13,14] (e.g., $T = 140$ °C and $P = 150$ MPa for PVDF[13]) or heterogeneous conditions[14−18] (e.g., $T < 80$ °C and $P < 40$ MPa for PVDF). However, most of the recent studies on VDF[15,19−23] and VDF−HFP[16,17] radical polymerization in supercritical medium involve heterogeneous conditions because of the milder temperature and pressure. In addition, depending upon type and amount of the selected stabilizer, two process modes are usually established: precipitation[15,17,20] or dispersion.[16,21−23] In both cases, the particle formation stage (nucleation) is completed within the first few minutes of reaction,[17,24] when monomer conversion is quite low. After the nucleation stage, the precipitated polymer particles may undergo a coagulation process, leading to the formation of large, irregular-shaped aggregates in the case of precipitations or to well-defined, micrometer-sized spherical particles when a suitable surfactant is used (dispersions).

In spite of the large body of reported experimental studies, crucial aspects of the heterogeneous copolymerization kinetics of VDF−HFP in $scCO_2$ are still under debate, mainly for what concern the contribution of each phase as reaction locus. In particular, with reference to VDF precipitation, it has been observed by independent groups[15,20] that bimodal molecular weight distributions (MWDs) are obtained at monomer concentration exceeding a threshold of about 2 mol/L. Bimodality was observed also in the case of VDF−HFP copolymers.[17] Different models have been proposed in the case of PVDF to explain such behavior, and the major contributions are briefly reviewed in the following.

A model presuming the polymerization reaction taking place exclusively in the continuous (CO_2-rich) phase was proposed by Saraf et al.,[15] who assumed that the increase in MWD polydispersity index (PDI) was due to chain transfer to polymer, thus leading to branching. Indeed, such a model was able to reproduce PDI experimental data, but the predicted MWDs remained monomodal in all cases. Later on, the same group proposed a different model taking into account the decrease in mobility of the macroradicals at increasing chain length, thus making the termination rate constant chain-length-dependent.[19] This way, the

*Corresponding author: e-mail galia@dicpm.unipa.it; Tel +39 091 23863758; Fax +39 091 7025020.

 Published on Web 11/12/2010

occurrence of the bimodality in MWD was well described. Finally, a further modification of the same one-phase model has been proposed very recently taking into account both chain transfer to polymer and diffusion-controlled termination at the same time.[25] The latter is assumed to take place when macroradical sizes exceed a critical value to be estimated by direct fitting to the experimental data.

As already mentioned, in all such models it was assumed that the whole process of radical generation, growth, and termination was occurring in the supercritical phase only (1-locus model). Differently, Mueller et al.[20] proposed a model that explains the two modes in the MWD as representative of polymer chains produced in the CO_2-rich, continuous phase and in the polymer-rich, dispersed phase (2-loci model). Monomer and initiator are partitioned between the two phases at equilibrium, while radicals, even if generated in the low-viscosity supercritical medium, can diffuse into the polymer phase before terminating and thus still be active. The rate of this mass transfer process is determining the relative amount of polymer produced in the two reaction loci. This quantity depends both on the relative amount of the two phases and on the polymer morphology: the smaller the polymer particles (and consequently the larger the total interphase area, A_p), the larger the contribution of the reaction in the polymer dispersed phase due to the enhanced capture of active chains from the continuous phase. Mueller et al.[20,21] showed that such a 2-loci model is able to predict the VDF homopolymerization kinetics under precipitation and dispersion conditions, i.e., with rather different total interphase area values, as well as the occurrence of MWD bimodality by minimal parameter adjustment.

Despite the very different mechanistic picture proposed, both the 1-locus and 2-loci models were able to describe bimodal MWDs, so that the real mechanism is still unclear. It is evident that a correct understanding of the role of each reaction locus has not only a fundamental but also a practical relevance because it is crucial for suitable process design and operation, especially in view of industrial scale production. Accordingly, the aim of this work is to find out whether the heterogeneous copolymerization of VDF and HFP in $scCO_2$ occurs only in one or in both phases and, in the latter case, to identify and clarify the contribution of each phase as reaction locus. The study was performed using experimental, model-independent evidence mainly based on the analysis of the final copolymer properties. In particular, the effects of polymer content and interphase area on the copolymer molecular weight distribution were considered. Polymer holdup was varied by carrying out batch reactions at increasing polymerization time. The effect of the total interfacial area, A_p, was studied by comparing precipitation and dispersion reactions. This experimental strategy was selected because any effect of the interfacial area (e.g., on the MWD) can be used to discriminate between the two mechanistic views. Indeed, from the viewpoint of the 1-locus models, no effect is expected by varying A_p because the particle phase is not involved in the polymerization process. On the other hand, in the frame of the 2-loci model, an increase of A_p enhances directly the interphase radical transport from the continuous to the particle phase and consequently increases the relative amount of polymer produced in the particle phase.[20,26]

2. Experimental Section

2.1. Materials. Vinylidene fluoride and hexafluoropropylene monomers supplied by Solvay Solexis and CO_2 by Air Liquide (99.998% pure) were used as received. The diethylperoxidicarbonate (DEPDC) initiator was synthesized with a procedure that was already described in the literature,[20] using water as solvent and extracting the initiator into Freon 113 (HPLC grade). The concentration of active peroxide in the solution was determined by the iodine titration technique, ASTM method E 298-91. All chemicals used in the synthesis of the DEPDC solution were obtained from Aldrich and used as received. The ammonium carboxylate perfluoropolyether salts FLK 7850A and FLK 7004A (general formula $[Cl-(CF_2CF(CF_3)O)_nCF_2COO^-]NH_4^+$ average molecular weight ca. 500 and 1000 g/mol, respectively) and Fomblin DA (general formula $[CF_3(CF_2CF(CF_3)O)_m(CF(CF_3)O)_n(CF_2O)_pCOO^-]NH_4^+$, average molecular weight ca. 3000 g/mol), all supplied by Solvay Solexis, were used as steric stabilizers because they were proven very effective in stabilizing PVDF dispersions.[21,22] The stabilizers had an initial water content ranging from 1 to 2% (w/w) and were used after drying in vacuum at 50 °C overnight.

2.2. Polymerization Apparatus and Reaction Procedure. Polymerization experiments were carried out in an AISI 316 batch reactor (ca. 27 mL), stirred by a magnetic bar and inserted in an automated temperature control system. The reactor was equipped with high-pressure valve (Parker), pressure transducer (Barksdale UPA3, estimated accuracy by calibration with a high-precision manometer of ±0.05 MPa), and Pt 100 temperature sensor (estimated accuracy of ±0.3 K). The experimental procedure adopted for VDF homopolymerization reactions is detailed elsewhere.[21] Dealing with copolymers, the loading procedure was modified as follows.

When used, a weighted amount of the surfactant was introduced in the reactor just after drying. Then the vessel was purged by a controlled flow rate of low-pressure gaseous CO_2 maintained for at least 15 min to remove air. The reactor was sealed, and the desired amount of monomers was added at room temperature. HFP was introduced first by heating its vessel using an electrical heating tape. VDF was pumped by a 250D ISCO syringe pump. The reactor was connected to monomer vessels by means of high-pressure tubes (1/8 in. o.d.) that were purged by flowing the corresponding monomer to remove air. The total amount of each monomer introduced was measured by weighing the vessel using an electronic balance (Sartorius, maximum 8 kg, precision 0.01 g). After loading the monomers, the reaction vessel was put into the temperature-controlled bath and heated at the reaction temperature ($T = 50$ °C). When the reactor reached the set-point temperature, the initiator solution was loaded in a sample loop of suitable volume and delivered inside the reactor by a stream of liquid CO_2 pumped by an air-driven Maximator pump up to the desired value of total pressure. The apparatus used to pump CO_2 and DEPDC into the reactor is represented in Scheme 1. The loading time of initiator and CO_2 was about 2−4 min, after which the reaction time was set to zero. When the desired reaction time was reached, the reactor was quenched by immersion in ice and water bath and slowly depressurized until venting of CO_2, VDF, and HFP was completed. Finally, the amount of copolymer formed was obtained by subtracting from the weight of the reactor measured after venting the weight of the empty reactor and of the (nonvolatile) surfactant loaded.

Before characterization, the copolymer obtained in the presence of surfactants was subjected to an extraction procedure with a controlled flow of $scCO_2$ at 40 °C and 20 MPa for 2 h (ISCO SFX 2-10 extractor) to remove the surfactant. This procedure proved to be effective for a quantitative recovery of the herein used stabilizers.[27] Comparison between GPC elution curves of extracted and untreated samples showed that the $scCO_2$ extraction process does not affect the polymer MWD (see Supporting Information).[28]

2.3. Polymer Characterization. Monomer conversion, X_w, was determined gravimetrically as the ratio between the mass of copolymer formed at the end of the polymerization experiments and the total mass of monomers fed into the reactor. The polymer volume fraction at the end of the reaction, ϕ_p, was estimated as

$$\phi_P = \frac{X_w M_0}{\rho_p V_R} \quad (1)$$

Scheme 1. (left) Sketch of the Experimental Apparatus Used To Feed CO_2 and DEPDC into the Batch Reactor and (right) Schematic Representation of the Switching Valve (V3)[a]

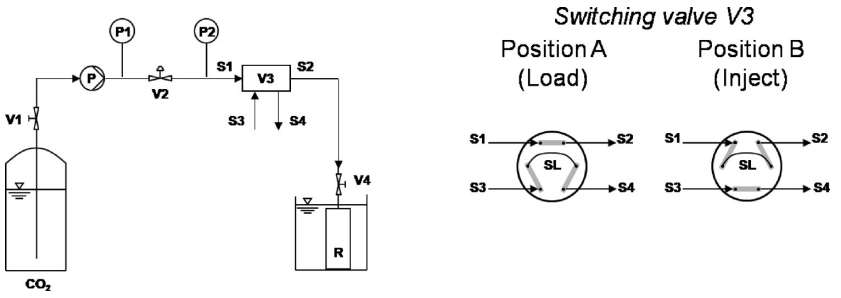

[a] V1, V4: valves; V2: reducing pressure regulator; V3: switching valve; P: air-driven pump; P1, P2 manometers; R: reactor; S1, S2: CO_2 stream line; S3, S4: stream line of DEPDC solution; SL: sampling loop. With V4 closed and V3 in position A, the CO_2 feed line is pressurized and the DEPDC solution is fed into the SL. Then V3 is switched to B, V4 is opened, and the CO_2 pumped into R through SL. When the desired pressure is reached, V4 is closed.

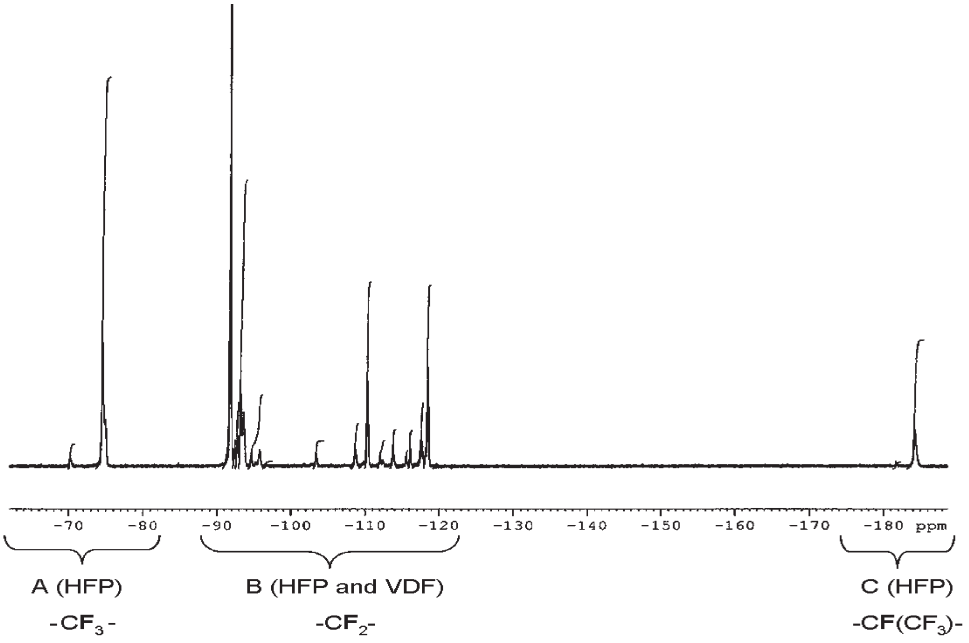

Figure 1. ^{19}F NMR spectrum of a P[VDF-*co*-HFP] sample polymerized at $T = 50$ °C in $scCO_2$. Data in the regions A, B, and C, indicated in the figure together with the corresponding repeating units, were used to estimate the average copolymer composition $\underline{F}_{HFP}$.

where M_0 is the total mass of monomers fed into the reactor, V_R is the reactor volume, and ρ_P is the density of the polymer. In eq 1 we used a constant value for copolymer density of $\rho_P = 1.75$ g/mL.[29] By this choice, any swelling of the polymer phase and any influence of temperature and pressure are neglected, and the value of ϕ_P has to be considered as a reasonable estimation.

The particle morphology was analyzed by a Philips scanning electron microscope (SEM) after sputter-coating the samples with gold.

The complete MWD was measured at 45 °C with a GPC instrument equipped with 2 × PL-Gel Mix-B LS columns as well as RI and viscosity detectors. These measurements were performed by preparing solutions of polymer samples at about 1.5 g/L in DMF (HPLC grade) modified with 1 g/L LiBr. Columns were calibrated using PMMA standards (M_p = 2680−3 900 000 g/mol; Polymer Laboratories. Ltd., UK). Online measurements of both RI and relative viscosity allowed the evaluation of the molecular weight distributions (MWDs) by the universal calibration approach.

^{19}F NMR spectra were measured in deuterated DMSO (ARMAR Chemicals) at 80 °C at 188 MHz with a Bruker instrument. Chemical shifts were related to the $CFCl_3$ signal at 0 ppm. A typical ^{19}F NMR spectrum for poly(VDF-*co*-HFP) is depicted in Figure 1. The detailed chemical shifts are available in the literature:[30,31] the groups of signal assigned to VDF repeat units are located at −91.4 to −96.2 ppm for head-to-tail normal additions (−CH_2C**F**$_2$−CH_2CF_2−), at −108.6 to −112.3 ppm for CF_2 groups adjacent to a HFP unit (−CH_2C**F**$_2$$CF_2$CF($CF_3$)−), and at −113.6 and −115.9 ppm for the head-to-head reversed addition (−CH_2C**F**$_2$−CF_2CH_2−). The groups of signal assigned to HFP units are centered at −70.3 and −75 ppm for the side CF_3 group (−CF_2CF(C**F**$_3$)−), at −115.3 and −117 to −119.2 ppm for the perfluoromethylene group in the HFP unit (−C**F**$_2$CF(CF_3)−), and at −181.4 and −184.1 ppm for the CF group (−CF_2C**F**(CF_3)−). Therefore, according to Beginn et al.,[17] the average HFP mole fraction incorporated in the copolymer, $\underline{F}_{HFP}$ is calculated by either one of the following equations:

$$\underline{F}_{HFP} = \frac{2C}{B} \tag{2}$$

$$\underline{F}_{HFP} = \frac{2A}{3B} \tag{3}$$

where A denotes the sum of the areas of NMR signals in the range from −70 to −76 ppm (CF_3 group), B from −91.4 to −119.2 ppm (CF_2 group), and C from −181.4 to −184.1 ppm (CF group).

Table 1. Main Characterization Results for the Copolymerization of VDF and HFP in $scCO_2$[a]

run	surfactant [g/L]	$f_{HFP,0}$ (mol %)	reaction time [min]	X_w (wt %)	$\underline{F}_{HFP}$ (mol %)	MW_n [kg/mol]	PDI	ϕ_p (%)
1	0	0	30−180	nonreproducible results; polymer not soluble				
2	0	21.5	60	8.7	6.7	74	2.7	2.3
3	0	20.0	180	23.9	7.1	98	2.9	5.8
4	0	20.6	360	41.5	7.9	104	3.1	10.9
5	0	28.6	30	4.3	9.4	67	1.7	1.3
6	0	30.0	120	14.4	10.7	73	2.1	4.1
7	3.6	0	180	43.8	0	77	35.5	8.8
8	17.6	0	69	41.2	0	102	3.2	7.7
9	18.4	0	180	60.8	0	137	3.6	12.2
10	17.8	15.2	180	30.8	4.9	131	3.0	7.5
11	17.7	20.5	60	6.2	6.3	85	2.0	1.5
12	17.7	22.6	180	18.2	7.1	152	2.3	4.8
13	18.4	21.4	360	35.5	7.1	160	2.5	9.4
14	18.0	30.0	30	4.5	10.2	67	1.5	1.3
15	17.9	28.2	120	15.6	9.2	94	2.3	4.6
16	18.3	30.0	180	21.6	9.9	97	2.2	6.1
17	17.6	43.3	180	12.3	15.7	83	1.8	4.4

[a] Operating conditions: $T = 50$ °C, $P_0 = 38.5$ MPa, [DEPDC] = 5.8 mM, monomer feed concentration [VDF] + [HDP] = 5.5 M. Operating conditions averaged over all batches. As surfactant, Fomblin was used for entry 7 and FLK-7004-A or FLK 7850-A for all other reactions.

Differences between $\underline{F}_{HFP}$ values obtained by the two equations were within 1%, and the average values were considered.

3. Effect of Monomer Feed Composition and Interphase Area

In order to study the effect of A_p on the copolymer MWD, it is first necessary to define experimental conditions in which either dispersion or precipitation polymerization takes place. In particular, if the surfactant is effective in stabilizing VDF−HFP copolymers, the first one occurs, thus ensuring higher values of the interphase area compared to the second. In a previous study on VDF homopolymerization,[22] it was shown that relatively high pressure ($P > 35$ MPa) and monomer concentration ($[VDF]_0 \cong 5.5$ mol/L) are necessary in order to achieve a stable dispersion when perfluoropolyether surfactants are used at $T = 50$ °C. This finding can be explained by the cumulative effect of increased solvency of the supercritical medium with density together with the cosolvent effect of the fluorinated monomer, which favor a more extended conformation of the perfluoropolyether tails, thus imparting more efficient steric stabilization.

Accordingly, several copolymerization reactions were carried out at increasing HFP comonomer initial mole fraction, $f_{HFP,0}$, and conditions similar to those leading to effective stabilization for PVDF dispersions. The selected experimental conditions are reported in the caption of Table 1, where the main characterization results are reported in terms of reaction time, final conversion (X_w), mole fraction of HFP in the final product ($\underline{F}_{HFP}$), and the corresponding number-average molecular weight (MW_n) and polydispersity (PDI). Note that the experimental runs are denoted as precipitation (runs 1−6) or dispersion (runs 7−17) polymerization depending on whether or not a surfactant was used and are then grouped together as a function of the initial feed HFP content ($f_{HFP,0}$).

As expected, the less reactive HFP[4] strongly affects the reaction rate as well as the weight-average molecular weights, which both decreased when the initial concentration of perfluorinated monomer was increased (for example, cf. in Table 1 conversion values, X_w, for dispersions at equal reaction time and increasing $f_{HFP,0}$, i.e., runs 9, 10, 12, 16, and 17).[28] Considering that termination is believed to occur predominantly by radical coupling,[15] relatively large values of the polydispersity index (PDI = MW_w/MW_n) were found in most cases.

3.1. Homopolymerization Reactions. Let us now examine the particle morphology and its relation with the MWD, which is the most relevant aspect in our study. The case of VDF homopolymerization is considered first. The surfactant-free VDF homopolymerization (precipitation) at monomer concentration of 5.5 M (Table 1, run 1) exhibited an irregular bulky structure (Figure 2a) and a nonreproducible kinetic behavior (Figure 3). Indeed, in repeated polymerization runs, we measured conversion values ranging from 24 to 57% at 1 h reaction time and from 44 to 68% at 3 h reaction time, indicating a loss of reaction control. Moreover, the collected dry product was extremely hard and not fully soluble in the GPC solvent, thus preventing its MWD analysis. Similar results are reported by Saraf et al.[15] for a continuous stirred tank reactor (CSTR) at about 6 M inlet monomer concentration: under these conditions, the reactor entered an "inoperability region", and after the reactor was shut down it was found filled with a hard-insoluble material.

When surfactant was added at concentration of 3.6 g/L (Table 1, run 7), corresponding to 1% w/w with respect to VDF, only partial stabilization of the polymer particles was achieved. The polymer exhibited both domains where microspherical particles were observed (Figure 2b) as well as domains with a morphology similar to that of precipitations (Figure 2a), thus corresponding to a larger interphase area compared to the case of precipitation reactions. In this case, the polymer was soluble in the GPC solvent, and the very distinct bimodality typical of VDF precipitation reactions when monomer concentration is higher than ca. 2−3 M[15,20] was measured. A further increase of surfactant concentration to 18 g/L (Table 1, runs 8 and 9) led to a polymer completely constituted by well-defined microspherical particles (Figure 2c) and therefore characterized by an even much larger interphase area. Again the collected polymer was fully soluble in the GPC solvent, and the conversion increased compared to the dispersion at lower interphase area (cf. Table 1, runs 7 and 9). More interestingly, the MWD was still broad but monomodal.

It is worth noting that all the above experimental findings are compatible with the existence of two reaction loci. Let us consider first the case in which the surfactant is effective, thus

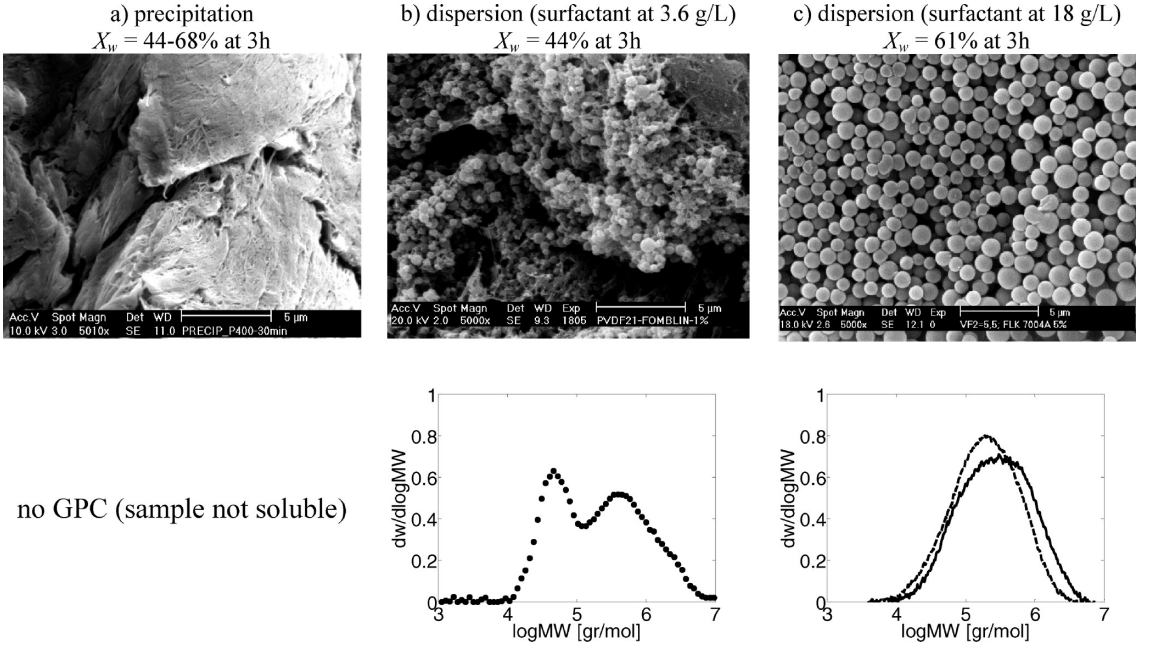

Figure 2. Effect of the surfactant concentration on the morphology and MWD of PVDF produced in $scCO_2$: (a) without surfactant (Table 1, run 1, SEM refers to 30 min reaction); (b) surfactant at 3.6 g/L, (Table 1, run 7); (c) surfactant at 18 g/L (Table 1, run 8, dashed line in the MWD; Table 1, run 9, SEM image and continuous line).

leading to dispersion polymerization (Figure 2c). In this case, the very high interphase area enhances the radicals interphase transport,[20] so that most of the growing radicals, poorly soluble in the continuous phase,[32] enter the polymer dispersed phase which therefore constitutes the main reaction locus. Accordingly, the resulting MWD exhibits a single mode in the high-MW region, representative of chains produced in the dispersed phase. At smaller A_p values (Figure 2b), the flow of radicals from the continuous to the dispersed phase is smaller. As a result, part of the radicals generated in the continuous phase terminate in the same phase before precipitating. In this case both phases are operative as reaction loci, each giving rise to its characteristic MWD mode, and the resulting overall MWD is bimodal.

Finally, the "inoperability" observed when working at even lower interphase area under precipitation polymerization conditions (Figures 2a and 3 and Saraf et al.[15]) can be better understood by considering the possible temperature increase in the polymer particles. For this, let us approximate a polymer aggregate with a sphere of radius r and thermal conductivity k and consider a uniform volumetric heat production rate inside the sphere, λ, due to the exothermal polymerization. Under these conditions, the temperature difference between the center of the particle ($T_{r=0}$) and its surface (T_S) is given by[33]

$$T_{r=0} - T_S = \frac{\lambda r^2}{6k} \tag{4}$$

The value of λ is given by the product of the heat of polymerization, ΔH_{pol}, times the average reaction rate (in the dispersed phase) per volume of polymer phase, and can be estimated as

$$\lambda = -\Delta H_{pol}\left(\frac{\alpha X_w [VDF]_0}{t_R \phi_p}\right) \tag{5}$$

where $X_w[VDF]_0$ represents the moles of VDF reacted per unit of reactor volume in the reaction time t_R and the factor

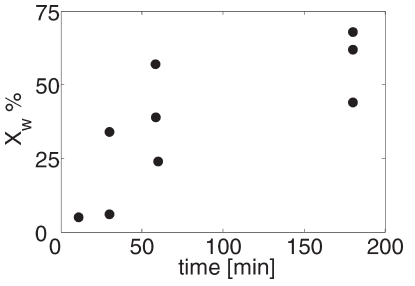

Figure 3. Conversion as a function of time for repeated precipitation polymerization runs of VDF (●, Table 1, run 1).

α is the fraction of them reacted in the dispersed phase, while ϕ_p is the polymer volume fraction in the reactor. For precipitations at initial monomer concentration exceeding 3 M, the amount of polymer produced in the dispersed phase is typically more than 50%, as estimated from the relative amount of the higher MW mode in the MWD.[15,20]

Accordingly we set $\alpha = 0.5$, and with $X_w = 0.24$ and $\phi_p = 0.048$ (corresponding to the lower conversion value measured for precipitations at $t_R = 60$ min, cf. Figure 3), we solved eq 4 with $\Delta H_{pol} = -474.2$ kJ/mol (at $T = 25$ °C)[2] and $k = 0.13$ W/mK.[34,35]

The calculated temperature difference between the center and the surface of the aggregates is plotted in Figure 4 versus the aggregate size, r. For small particles the temperature profile is flat (no temperature gradient), and the reaction in the polymer phase occurs under isothermal conditions (dispersions). But when aggregates exceed a size of a few millimiters (as in the case of precipitations in which bulky polymer is formed), the large amount of heat produced by the reaction causes a remarkable temperature increase in the particle core. Such local temperature increase promotes autoacceleration of the reaction in the polymer phase, eventually leading to loss of reaction control and formation of insoluble polymer due to enhanced chain transfer to polymer. Indeed, temperature promotes chain transfer to polymer

reaction[18] which, combined with termination by coupling, may form cross-linked and therefore insoluble molecules. Such picture is also consistent with the observation that no inoperability is observed for precipitations at low VDF loading.[15] Under dilute monomer conditions, the amount of polymer formed and the solubility of VDF in it are very low,[36] making the contribution of the polymer phase as reaction locus negligible, as indicated by the fact that the mode at high MW in the MWD disappears at decreasing VDF loading.[15,20] Futhermore, the lower polymer content in the reactor slows down the aggregation process. This way both λ and r remain small during the reaction time, and no inoperability is observed because of the achievement of isothermal conditions inside the polymer phase (eq 4).

3.2. Copolymerization Reactions. Let us now analyze the copolymerization reactions. No significant differences were observed between the two cases, precipitation and dispersion, in terms of reaction rate. SEM images revealed that for copolymers with $f_{HFP,0} \cong 0.2$ (Table 1, runs 4 and 13 and Figure 5) and $f_{HFP,0} \cong 0.3$ (Table 1, runs 6 and 15 and Figure 6) both dispersions and precipitations led to the formation of microparticles. Nevertheless, dispersions provided more segregated and well-defined particles compared to precipitations, for which particles were coalesced and irregularly shaped.

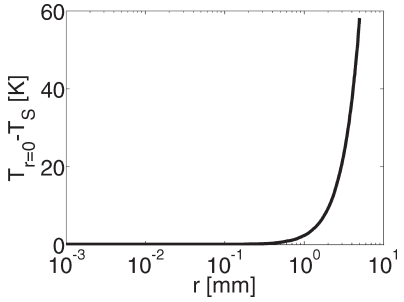

Figure 4. Calculated temperature difference between the center and the surface of a sphere in which an exothermic reaction occurs homogeneously as a function of the sphere size (eq 4).

From image analyses we could estimate that the average size of the aggregates in the case of precipitations was about 2−3 times larger than in the corresponding dispersions. This, for the same total polymer volume, implies about 10−30 times less particles and A_p values smaller by a factor 2−3. It is worth noting that, at values of temperature and pressure close to those considered here and up to $f_{HFP,0} \cong 0.30$, independent groups have shown that the copolymer is essentially insoluble in the reaction medium and precipitates out of the supercritical phase just after the first few minutes of reaction.[14,17] Therefore, at the operating conditions under examination, the system is below the copolymer cloud point, and we are still dealing with heterogeneous reactions.

With respect to the effect of the interfacial area on the MWD, the same differences as in the homopolymer case were observed at $f_{HFP,0} \cong 0.2$. In particular, as shown in Figure 7 (Table 1, runs 4 and 13), bimodal and monomodal MWDs were measured for precipitation and dispersion polymerization, respectively. Figure 8 shows a comparison of the MWDs measured in runs 6 and 15 of Table 1 at $f_{HFP,0} \cong 0.3$: the tail or shoulder in the region of the high molecular weights is observed in both cases, with again the relevance of the high-MW region increasing at increasing interphase area A_p. These experimental findings again indicate that the polymer morphology, the only relevant difference between the two sets of examined polymerization runs, strongly affects the final MWD: once again, such behavior is consistent with a 2-loci model and not with a homogeneous model. Note that, since even precipitations led to micrometer-sized aggregates, according to the results in Figure 4, no inoperability was observed in the case of copolymerization reactions, in agreement with previous literature results.[16,17]

Finally, when $f_{HFP,0}$ reached the value of 0.43 and the corresponding copolymer composition was $\underline{F}_{HFP} = 0.16$

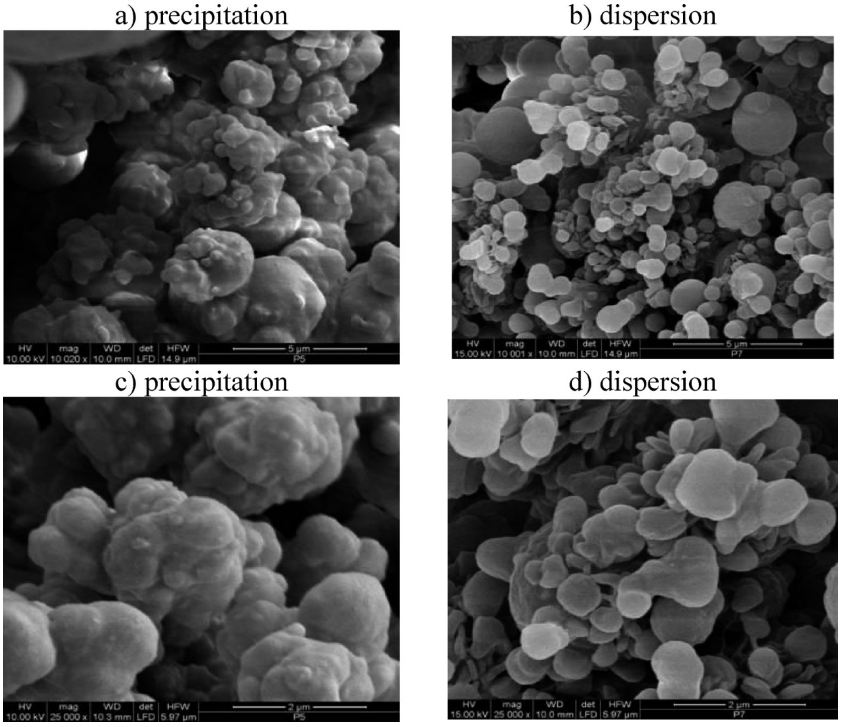

Figure 5. Effect of the surfactant concentration on the copolymer morphology for reactions with initial monomer composition $f_{HFP,0} \cong 0.2$: (a, c) precipitation (Table 1, run 4); (b, d) dispersion (Table 1, run 13).

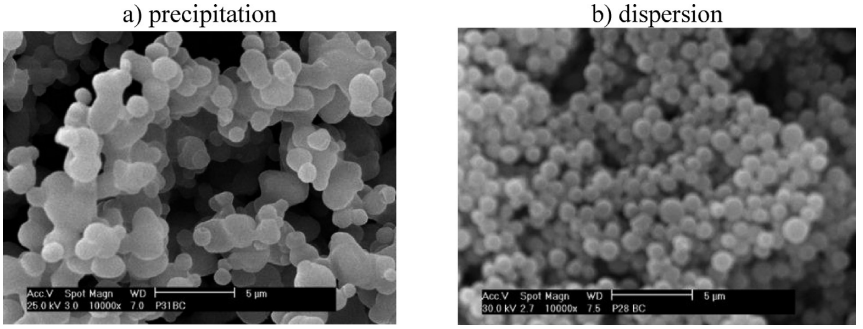

Figure 6. Effect of the surfactant concentration on the copolymer morphology for reactions with initial monomer composition $f_{HFP,0} \cong 0.3$: (a) precipitation (Table 1, run 6); (b) dispersion (Table 1, run 15).

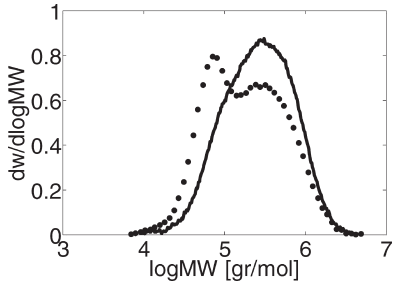

Figure 7. Effect of the interphase area, A_p, on the measured molecular weight distribution for samples produced at initial monomer composition $f_{HFP,0} \cong 0.2$ under precipitation (●, Table 1, run 4) and dispersion conditions (continuous line, Table 1, run 13).

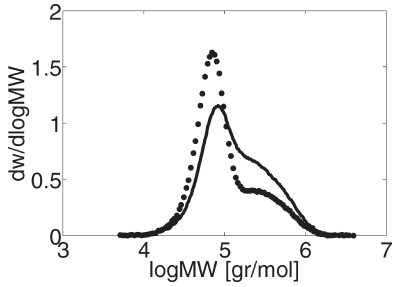

Figure 8. Effect of the interphase area, A_p, on the measured molecular weight distribution for samples produced at initial monomer composition $f_{HFP,0} \cong 0.3$ under precipitation (●, Table 1, run 6) and dispersion conditions (continuous line, Table 1, run 15).

(Table 1, run 17), the polymer particles were completely coalesced also when surfactant was used (Figure 9a), and the effect of the interfacial area on the copolymer molecular weight distribution could not be assessed anymore. This dramatic change in the product morphology can be tentatively attributed to the cooperative effect of the enhanced solubility of CO_2 (in the amorhpous fraction of the copolymer) and of the decreased crystallinity[28] at increasing HFP content: the plasticization effect induced by sorption softens the polymer phase which becomes more similar to an expanded, liquidlike polymer rather than to a solid matrix. Indeed, when contacting with $scCO_2$, a commercial copolymer ($F_{HFP} = 0.22$, $X_{cr} = 0$), we observed that the sample exhibited a liquidlike behavior already at mild temperature and pressure conditions, as shown in Figure 9b, in contrast to the case of the VDF homopolymer, which remains solid and rigid.[37]

To summarize, in reaction systems where the presence of a stabilizer allowed the development of enough interfacial area, we observed an increase of the amount of polymer chains at higher molecular weight. This indicates that A_p affects the reaction progress of the system and is consistent with the picture provided by a 2-loci reaction model. Furthermore, the inoperability region observed when carrying out VDF precipitation reactions at high monomer loading disappears at increasing interphase area: this behavior is not compatible with the hypothesis of polymerization occurring only in the supercritical phase, while it can be explained by the 2-loci model as loss of reaction control due to nonisothermal conditions in the polymer particles when large aggregates are formed.

4. Effect of Polymer Holdup on Molecular Weight Distribution

In order to better elucidate the effect of the particle surface area, A_p, on the systems behavior, the MWDs normalized to the copolymer conversion (that is, with area proportional to the total mass of produced copolymer) are represented at increasing reaction time and therefore at increasing polymer holdup, ϕ_p, in Figures 10 and 11 for precipitation and dispersion polymerizations, respectively.

In the case of precipitation reactions (Figure 10) at short polymerization time and low ϕ_p, the MWDs exhibit a dominant low-MW peak with some tailing in the high-MW region at $f_{HFP} \cong 0.2$ (Figure 10a) as well as at $f_{HFP} \cong 0.3$ (Figure 10b). At increasing reaction time and ϕ_p, the second mode in the high-MW region becomes more visible in both cases, even though the low-MW peak remains the dominant one. The MWD profiles for dispersions, shown in Figure 11, are very similar to those observed for precipitations at the shortest reaction time. However, at longer reaction times, the high-MW shoulder becomes the dominant one, eventually leading to very broad but still monomodal MWDs.

Also, the MWDs evolution with time (larger reaction times correspond to larger polymer holdups, ϕ_p, in Figures 10 and 11) is consistent with a 2-loci model, being low- and high-MW peaks associated with the polymer formed in the continuous and dispersed phase, respectively. In all cases, at low conversion the small polymer amount (ϕ_p smaller than 2.5%) collects only a small fraction of the growing radicals, and the continuous phase is the main reaction locus. At increasing time and polymer holdup, the dispersed phase increases its relevance as reaction locus (the fraction of the higher MW mode increases) and eventually becomes the predominant one. Under otherwise constant conditions, this evolution is regulated by the amount of available interphase area, A_p, which controls the transfer of the radicals from the continuous to the particulate phase. Since precipitation polymerization exhibits lower A_p values, this transition is much slower, and in fact even at the highest ϕ_p value in Figure 10a the contributions of the two reaction loci are still comparable and the corresponding MWD is still bimodal.

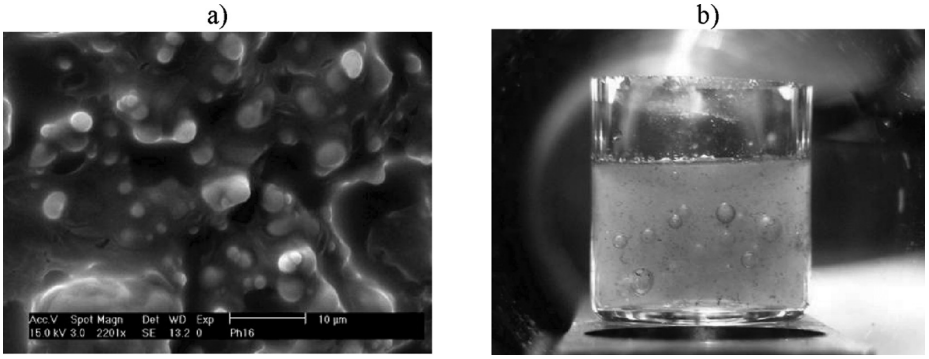

Figure 9. (a) SEM image of a sample produced by dispersion polymerization with initial monomer composition $f_{HFP,0} = 0.43$ (Table 1, run 17). (b) Picture of a commercial copolymer (Tecnoflon N 935 from Solvay-Solexis, $F_{HFP} = 0.22$, $MW_n = 110$ kg/mol) contacted with CO_2 at $T = 50$ °C and $P < 140$ bar. Complete melting of the copolymer sample is demonstrated by the formation of well visible CO_2 bubbles when the cell was slowly depressurized from $P = 140$ bar to $P = 115$ bar.

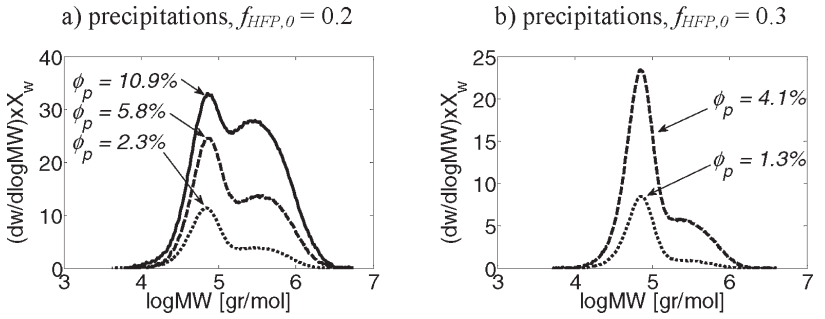

Figure 10. Effect of reaction time and polymer holdup, ϕ_p, on molecular weight distributions for samples produced under precipitation conditions: (a) initial monomer composition $f_{HFP,0} \cong 0.2$ (Table 1, runs 2−4); (b) initial monomer composition $f_{HFP,0} \cong 0.3$ (Table 1, runs 5 and 6).

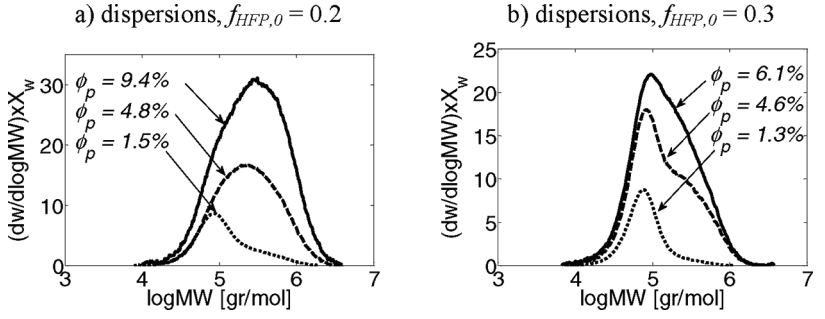

Figure 11. Effect of reaction time and polymer holdup, ϕ_p, on molecular weight distributions for samples produced under dispersion conditions: (a) initial monomer composition $f_{HFP,0} \cong 0.2$ (Table 1, runs 11−13); (b) initial monomer composition $f_{HFP,0} \cong 0.3$ (Table 1, runs 14−16).

The analysis above actually explains also the experimental results reported by Ahmed et al.[38] Those experiments were actually designed in order to discriminate among continuous, interfacial, or polymer particle reaction locus. But according to our results, the real scenario is somehow more complex than those considered by Ahmed et al.[38] Indeed, there is not a single reaction site all along the reaction but a gradual transition from one site (continuous phase) to the other (dispersed phase). In particular, the cited authors analyzed the effect of the polymer holdup on precipitation copolymerization kinetics in a continuous stirred tank reactor up to ϕ_p values of about 2.5%. As shown in Figure 10, under these conditions the contribution of the continuous phase to the overall polymerization still prevails over the one of the polymer particles, and the corresponding data do not allow to detect the role of the dispersed phase as site of polymerization. Indeed, in these conditions a 1-locus polymerization model is expected to provide good predictions in terms of average properties (reaction rate and number-average molecular weight), as shown by Ahmed et al.[38]

5. Copolymer Composition

For an homogeneous system, the "instantaneous" composition of the copolymer, F_{HFP}, is directly related to the composition of the monomer mixture producing it through the Mayo−Lewis equation:[39]

$$F_{HFP} = \frac{r_{HFP} f_{HFP}^2 + f_{VDF} f_{HFP}}{r_{HFP} f_{HFP}^2 + 2 f_{VDF} f_{HFP} + r_{VDF} f_{VDF}^2} \qquad (6)$$

where r_{VDF} and r_{HFP} are the reactivity ratios of the two monomers defined as the ratios of the propagation rate constants:

$$r_{VDF} = \frac{k_{pVDF-VDF}}{k_{pVDF-HFP}}; \quad r_{HFP} = \frac{k_{pHFP-HFP}}{k_{pHFP-VDF}} \qquad (7)$$

Therefore, since the reaction can occur in both phases, differences in copolymer composition could in principle be observed when moving from precipitation to dispersion regimes if the two phases are characterized by different reactivity ratios or monomer compositions.

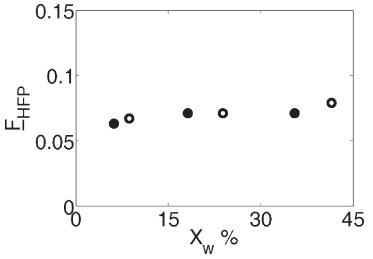

Figure 12. Drift of average copolymer composition as a function of conversion for precipitation (○) and dispersion (●) copolymerization of VDF and HFP in $scCO_2$ at $f_{HFP,0} \cong 0.2$ (Table 1, runs 2−4 and 11−13, respectively).

This way, copolymer composition also could be used to detect the main reaction locus.[40]

For the copolymerization reaction of VDF and HFP, the reactivity ratios reported in the literature for aqueous emulsion/suspension or acetonitrile solution polymerization are in the range $r_{VDF} = 2.5-6.7$ and $r_{HFP} \approx 0-0.1$,[4] which are very similar to those reported for reactions in $scCO_2$, i.e., $r_{VDF} = 3.6-5.1$ and $r_{HFP} \approx 0-0.1$.[14,16,17,41] It is thus reasonable to expect similar reactivity ratios in the two phases. In this case a different composition of the two monomers in the continuous and dispersed phase is the essential prerequisite to detect a change of the main reaction locus from the drift of the copolymer composition.

Figure 12 reports the average $\underline{F}_{HFP}$ measured by ^{19}F NMR for precipitation (empty symbols) and dispersion (filled symbols) reactions as a function of conversion with initial HFP mole fractions $f_{HFP,0}$ of about 0.2. The composition drift with conversion was limited to values lower than a few percent, and no significant change in $\underline{F}_{HFP}$ was observed when the main reaction locus was changed from the homogeneous to the dispersed phase by increasing polymer holdup and A_p. We can conclude that polymer chains have similar instantaneous composition in both reaction phases. This observation implies that, under the selected operative conditions, the monomer composition is not significantly different in the continuous and in the dispersed phase, and the copolymer composition cannot be used to clearly identify the main reaction locus.

6. Conclusions

When the copolymerization of VDF and HFP was performed in $scCO_2$ in the presence of ammonium carboxylate perfluoropolyether surfactants and HFP mole fraction in the feed ranging from 0 to 0.3, the formation of polymer particles was observed. The corresponding increase of total interphase area, A_p, enhanced the kinetics of radical transport and the contribution of the polymer phase as reaction locus compared to precipitation reactions with much smaller A_p. The significant MWD changes when polymer holdup and A_p were increased clearly indicate that the polymerization started in all cases in the supercritical phase, but it quickly shifted to the polymer phase provided that enough interface area became available. The MWD of the final product reflected the relative contribution of both loci. Indeed, under the experimental conditions considered in this work, longer polymer chains were produced in the dispersed phase compared to those produced in the continuous phase, leading to bimodal or monomodal MWD for precipitation or dispersion reactions, respectively.

Therefore, even though 1-locus models can be used at low conversion values when polymer holdups smaller than a few percent are reached, the same models cannot cover the whole process because they do not account for the effect of the interfacial area on the final molecular weight distribution. According to the reported experimental evidence, the general 2-loci polymerization scheme previously proposed by Mueller et al.[20] for precipitation/dispersion reactions in supercritical carbon dioxide applies to both VDF homopolymerization and its copolymerization with HFP up to initial HFP feed mole fractions of 0.30. Above this value, the plasticization effect caused by the CO_2 sorption softened the copolymer, causing particle coalescence, and thus prevented to study the effect of the interfacial area on the MWD.

From the 2-loci model perspective, the loss of reaction control observed for VDF precipitation reactions occurring at high monomer loading is due to nonisothermal conditions inside the polymer dispersed phase when large aggregates are formed. The consequent reactor inoperability is overcome by carrying out reactions in which smaller aggregates are produced, e.g., under dispersion conditions.

Acknowledgment. The financial support of Università di Palermo is gratefully acknowledged. We gratefully thank Paolo Guerra (Università di Palermo), Martin Colussi (ETHZ), Doris Sutter (ETHZ), and Thomas-B. Schweizer (ETHZ) for their valuable technical assistance.

Supporting Information Available: Supplementary figures showing the effect of HFP monomer feed composition on conversion and copolymer molecular weight, the effect of HFP incorporation on the copolymer crystallinity degree, and representative GPC elution profiles of VDF−HFP copolymers polymerized in $scCO_2$. This material is available free of charge via the Internet at http://pubs.acs.org.

References and Notes

(1) Ebnesajjad, S.; Khaladkar, P. R. *Fluoropolymers Applications in Chemical Processing Industries - The Definitive User's Guide and Databook*; William Andrew Publishing: Norwich, NY, 2005.
(2) Albert, L. M. *Fluoroelastomers Handbook - The Definitive User's Guide and Databook*; William Andrew Publishing: Norwich, NY, 2006.
(3) Giannetti, E. *Polym. Int*. **2001**, *50*, 10–26.
(4) Ameduri, B.; Boutevin, B.; Kostov, G. *Prog. Polym. Sci*. **2001**, *26*, 105–187.
(5) Ameduri, B. *Chem. Rev*. **2009**, *109*, 6632–6686.
(6) Pluskal, M. G.; Przekop, M. B.; Kavonian, M. R.; Vecoli, C.; Hicks, D. A. *Biotechnology* **1986**, *4*, 272–283.
(7) Bronstein, I.; Voyta, J. C.; Murphy, O. J.; Bresnick, L.; Kricka, L. J. *Biotechnology* **1992**, *12*, 748–753.
(8) Soresi, B.; Quartarone, E.; Mustarelli, P.; Magistris, A.; Chiodelli, G. *Solid State Ionics* **2004**, *166*, 383–389.
(9) Kim, J. R.; Choi, S. W.; Jo, S. M.; Lee, W. S.; Kim, B. C. *J. Electrochem. Soc*. **2005**, *152*, A295–A300.
(10) Cooper, A. I. *J. Mater. Chem*. **2000**, *10*, 207–234.
(11) McCoy, M. *Chem. Eng. News* **1999**, *77*, 11–13.
(12) *Chem. Eng. News* **2002**, *80*, 17−18.
(13) Beuermann, S.; Imran-Ul-Haq, M. *J. Polym. Sci., Part A: Polym. Chem*. **2007**, *45*, 5626–5635.
(14) Ahmed, T. S.; DeSimone, J. M.; Roberts, G. W. *Macromolecules* **2006**, *39*, 15–18.
(15) Saraf, M. K.; Gerard, S.; Wojcinski, L. M.; Charpentier, P. A.; DeSimone, J. M.; Roberts, G. W. *Macromolecules* **2002**, *35*, 7976–7985.
(16) Tai, H.; Wang, W.; Howdle, S. M. *Macromolecules* **2005**, *38*, 9135–9142.
(17) Beginn, U.; Najjar, R.; Ellmann, J.; Vinokur, R.; Martin, R.; Moller, M. *J. Polym. Sci., Part A: Polym. Chem*. **2006**, *44*, 1299–1316.
(18) Galia, A.; Caputo, G.; Spadaro, G.; Filardo, G. *Ind. Eng. Chem. Res*. **2002**, *41*, 5934–5940.
(19) Ahmed, T. S.; DeSimone, J. M.; Roberts, G. W. *Chem. Eng. Sci*. **2004**, *59*, 5139–5144.
(20) Mueller, P. A.; Storti, G.; Morbidelli, M.; Apostolo, M.; Martin, R. *Macromolecules* **2005**, *38*, 7150–7163.
(21) Mueller, P. A.; Storti, G.; Morbidelli, M.; Costa, I.; Galia, A.; Scialdone, O.; Filardo, G. *Macromolecules* **2006**, *39*, 6483–6488.
(22) Galia, A.; Giaconia, A.; Scialdone, O.; Apostolo, M.; Filardo, G. *J. Polym. Sci., Part A: Polym. Chem*. **2006**, *44*, 2406–2418.

(23) Tai, H.; Wang, W.; Howdle, S. M. *Macromolecules* **2005**, *38*, 1542–1545.
(24) Fehrenbacher, U.; Ballauff, M. *Macromolecules* **2002**, *35*, 3653–3661.
(25) Ahmed, T. S.; DeSimone, J. M.; Roberts, G. W. *Chem. Eng. Sci.* **2010**, *65*, 651–659.
(26) Mueller, A. P.; Storti, G.; Morbidelli, M.; Mantelis, C. A.; Meyer, T. *Macromol. Symp.* **2007**, *259*, 218–225.
(27) Scialdone, O.; Galia, A.; Raimondi, S.; Filardo, G. *J. Supercrit. Fluids* **2007**, *39*, 347–353.
(28) See Supporting Information.
(29) Mekhilef, N. *J. Appl. Polym. Sci.* **2001**, *80*, 230–241.
(30) Pianca, M.; Bonardelli, P.; Tatò, M.; Cirillo, G.; Moggi, G. *Polymer* **1987**, *28*, 224–230.
(31) Isbester, P. K.; Brandt, J. L.; Kestner, T. A.; Munson, E. J. *Macromolecules* **1998**, *31*, 8192–8200.
(32) Bonavoglia, B.; Storti, G.; Morbidelli, M. *Ind. Eng. Chem. Res.* **2006**, *45*, 3335–3342.
(33) Bird, R. B.; Stewart, W. E.; Lightfoot, E. N. *Transport Phenomena*, 2nd ed.; John Wiley & Sons: New York, 2002.
(34) Barros Melo, W. L.; Faria, R. M. *Appl. Phys. Lett.* **1995**, *67*, 3892–3894.
(35) Bonno, B.; Laporte, J. L.; Tascón d'León, R. *Meas. Sci. Technol.* **2001**, *12*, 671–675.
(36) Galia, A.; Cipollina, A.; Scialdone, O.; Filardo, G. *Macromolecules* **2008**, *41*, 1521–1530.
(37) Briscoe, B. J.; Lorge, O.; Dang, P. *Philos. Mag.* **2002**, *82*, 2081–2091.
(38) Ahmed, T. S.; DeSimone, J. M.; Roberts, G. W. *Macromolecules* **2009**, *42*, 148–155.
(39) Odian, G. *Principles of Polymerization*, 4th ed.; John Wiley & Sons: New York, 2004.
(40) Nomura, M.; Satpathy, U. S.; Kouno, Y.; Fujita, K. *J. Polym. Sci., Part C: Polym. Lett.* **1988**, *26*, 385–390.
(41) Möller, E.; Schreiber, U.; Beuermann, S. *Macromol. Symp.* **2010**, *289*, 52–63.